Arch Toxicol (2010) 84:631–640
DOI 10.1007/s00204-010-0526-8

ORGAN TOXICITY AND MECHANISMS

Pyrogallol-induced As4.1 juxtaglomerular cell death is attenuated by MAPK inhibitors via preventing GSH depletion

Yong Hwan Han · Woo Hyun Park

Received: 5 November 2009 / Accepted: 9 February 2010 / Published online: 27 February 2010

Abstract Pyrogallol (PG) induces apoptosis in several types of cells mediated by superoxide anion ($O_2^{\bullet-}$). Here, we investigated the effects of PG and/or MAPK (MEK, JNK, and p38) inhibitors on the changes in cell growth, cell death, reactive oxygen species (ROS), and GSH levels in As4.1 juxtaglomerular (JG) cells. PG inhibited the growth of As4.1 cells. It also induced apoptosis and the loss of mitochondrial membrane potential (MMP; $\Delta\Psi_m$) and increased the level of p53 protein. Intracellular $O_2^{\bullet-}$ level was increased in PG-treated As4.1 cells. PG also increased the number of GSH deleted cells in As4.1 cells. All the MAPK inhibitors significantly attenuated the growth inhibition and death mediated by PG. They decreased the levels of p53 protein and MMP ($\Delta\Psi_m$) loss in PG-treated As4.1 cells. They also reduced $O_2^{\bullet-}$ level and GSH-depleted cell number in these cells. In conclusion, MAPK inhibitors attenuated As4.1 cell growth inhibition and death mediated by PG treatment. The changes in $O_2^{\bullet-}$ and GSH levels by PG and/or MAPK inhibitors appeared to affect the growth and death of As4.1 cells.

Keywords Pyrogallol · Apoptosis · As4.1 · MAPK · ROS · GSH

Abbreviations

PG	Pyrogallol
ROS	Reactive oxygen species
MAPK	Mitogen-activated protein kinase
MEK	MAP kinase or ERK kinase
ERK	Extracellular signal-regulated kinase
JNK	c-Jun N-terminal kinase
SOD	Superoxide dismutase
MMP ($\Delta\Psi_m$)	Mitochondrial membrane potential
FBS	Fetal bovine serum
FITC	Fluorescein isothiocyanate
H_2DCFDA	2′,7′-Dichlorodihydrofluorescein diacetate
DHE	Dihydroethidium
GSH	Glutathione
CMFDA	5-Chloromethylfluorescein diacetate
MTT	3-(4,5-Dimethylthiazol-2-yl)-2,5-diphenyltetrazolium bromide
PI	Propidium iodide

Y. H. Han · W. H. Park (✉)
Department of Physiology, Medical School,
Chonbuk National University,
JeonJu 561-180, Republic of Korea
e-mail: parkwh71@chonbuk.ac.kr

Introduction

Pyrogallol (PG), a polyphenol, is a well-known superoxide anion ($O_2^{\bullet-}$) generator (Saeki et al. 2000; Yamada et al. 2003). It has often been used to investigate the role of $O_2^{\bullet-}$ in biological systems. The $O_2^{\bullet-}$ belongs to the reactive oxygen species (ROS) including hydrogen peroxide (H_2O_2) and hydroxyl radical ($^{\bullet}OH$). ROS have recently been implicated in the regulation of many important cellular events, including transcription factor activation, gene expression, differentiation, and cell proliferation (Baran et al. 2004; Bubici et al. 2006). ROS are formed as by-products of mitochondrial respiration or certain oxidases (Zorov et al. 2006). A change in the redox state of the tissue implies a change in the generation or metabolism of ROS. The principal metabolic pathways include superoxide dismutase (SOD), expressed as extracellular, cytoplasmic, and mitochondrial isoforms (Zelko et al. 2002), which metabolizes $O_2^{\bullet-}$ to H_2O_2. Further metabolism by

peroxidases, including catalase and glutathione (GSH) peroxidase, yields O_2 and H_2O (Wilcox 2002). Cells possess antioxidant systems to control the redox state, which is important for their survival. Excessive production of ROS gives rise to the activation of events leading to death in several cell types (Simon et al. 2000; Chen et al. 2006; Dasmahapatra et al. 2006; Wallach-Dayan et al. 2006). Also, PG has been shown to induce the $O_2^{\bullet-}$-mediated death of several types of cell such as mesangial cells (Moreno-Manzano et al. 2000), human lymphoma cells (Saeki et al. 2000), human glioma cells (Sawada et al. 2001), and Calu-6 lung cancer cells (Han et al. 2008c, 2009).

The mitogen-activated protein kinases (MAPKs) are a large family of serine/threonine kinases, which are major components of signaling pathways in cell proliferation, differentiation, and cell death (Blenis 1993). There are currently three well-known MAPKs: the extracellular signal-regulated kinase (ERK1/2), the c-Jun N-terminal kinase/stress-activated protein kinase (JNK/SAPK), and the p38 (Genestra 2007). Each MAP kinase pathway has relatively different upstream activators and specific substrates (Kusuhara et al. 1998). Numerous evidence demonstrates that JNK and p38 are strongly activated by ROS or by a mild oxidative shift of the intracellular thiol/disulfide redox state, leading to apoptosis (Gomez-Lazaro et al. 2007; Nagai et al. 2007; Hsin et al. 2008; Mao et al. 2008). ROS are also known to induce ERK phosphorylation and activate the ERK pathway (Guyton et al. 1996). In most instances, ERK activation has a pro-survival function rather than pro-apoptotic effects (Henson and Gibson 2006; Rygiel et al. 2008). Since different ROS levels and diverse functions of MAPKs by ROS may have opposite effects even in the same type of cells, the relationship between ROS and MAPKs in view of cell survival or cell death signaling needs further clarification.

Juxtaglomerular cell tumors (reninomas) are rare benign tumors of the kidney, with only about 100 cases having been described to date. Reninomas are understood to arise from juxtaglomerular (JG) cells, for which As4.1 cells have been used as a model (Sigmund et al. 1990). We recently demonstrated that PG inhibited the growth of As4.1 cells and induced apoptosis in these cells (Park et al. 2007a), and PG-induced apoptosis in As4.1 cells is correlated with the changes in GSH levels (Park et al. 2007b). However, little is known about relationships between ROS level and MAPK signaling in PG-treated As4.1 cells. Therefore, in the present study, we investigated the effects of PG and/or MAPK (MEK, JNK, p38) inhibitors on the changes in cell growth, cell death, reactive oxygen species (ROS), and GSH levels in As4.1 cells.

Materials and methods

Cell culture

As4.1 cells were obtained from the American Type Culture Collection (ATCC, Rockville, MD, USA) and maintained in a humidified incubator containing 5% CO_2 at 37°C. As4.1 cells were cultured in DMEM supplemented with 10% fetal bovine serum (FBS) and 1% penicillin–streptomycin (GIBCO BRL, Grand Island, NY). Cells were routinely grown in 100-mm plastic tissue culture dishes (Nunc, Roskilde, Denmark).

Reagents

PG was purchased from the Sigma–Aldrich Chemical Company (St. Louis, MO). PG was dissolved in H_2O at 100 mM as a stock solution. JNK inhibitor (SP600125), MEK inhibitor (PD98059), and p38 inhibitor (SB203580) were purchased from Calbiochem (San Diego, CA). These agents were dissolved in DMSO solution at 10 mM as a stock solution. Cells were pretreated with each MAPK inhibitor for 30 min prior to treatment with PG. Based on previous experiments, 50 μM PG was chosen as a suitable dose to differentiate the levels of cell growth inhibition or death in the presence or absence of each MAPK inhibitor. The dose of 10 μM each MAPK inhibitor was used as an optimal dose in this experiment. DMSO (0.2%) was used as a control vehicle. All stock solutions were wrapped in foil and kept at −20°C.

Cell growth and cell count assay

The effect of drugs on As4.1 cell number and growth was determined by trypan blue cell counting or by measuring 3-(4,5-dimethylthiazol-2-yl)-2,5-diphenyltetrazolium bromide (MTT) dye absorbance by living cells, as previously described (Park et al. 2000). In brief, 2×10^5 cells per well were seeded in 24-well plates (Nunc) for cell counting, and 5×10^3 cells per well were seeded in 96-well microtiter plates (Nunc) for MTT assays. After exposure to 50 μM PG with or without a given MAPK inhibitor for 72 h, cells in 24-well plates were collected with trypsin digestion for trypan blue cell counting, and cells in 96-well plates were used for an MTT assay. Twenty microliters of MTT (Sigma) solution (2 mg/ml in PBS) was added to each well of the 96-well plates. The plates were incubated for 4 additional hours at 37°C. Medium in plates was withdrawn using pipetting, and 200 μl DMSO was added to each well to solubilize the formazan crystals. Optical density was measured at 570 nm using a microplate reader (Spectra MAX 340, Molecular Devices Co, Sunnyvale, CA).

Cell cycle and Sub-G1 analysis

The cell cycle distributions and sub-G1 cells were determined by propidium iodide (PI, Sigma–Aldrich; Ex/Em = 488 nm/617 nm) staining, as previously described (Han et al. 2008c). In brief, 1×10^6 cells in 60-mm culture dish (Nunc) were incubated with 50 μM PG with or without a given MAPK inhibitor for 72 h. Cells were then washed with PBS and fixed in 70% ethanol. Cells were washed again with PBS, then incubated with PI (10 μg/ml) with simultaneous RNase treatment at 37°C for 30 min. Cell DNA content was measured using a FACStar flow cytometer (Becton–Dickinson, San Jose, CA).

Western blot analysis

The expressions of proteins were evaluated using Western blot analysis, as previously described (Han et al. 2008b). In brief, 1×10^6 cells in 60-mm culture dish (Nunc) were incubated with 50 μM PG with or without a given MAPK inhibitor for 1 or 72 h. The cells were then washed in PBS and suspended in five volumes of lysis buffer (20 mM HEPES. pH 7.9, 20% glycerol, 200 mM KCl, 0.5 mM EDTA, 0.5% NP40, 0.5 mM DTT, and 1% protease inhibitor cocktail). Lysates were then collected and stored at −20°C until further use. Supernatant protein concentrations were determined using the Bradford method. Supernatant samples containing 40 μg total protein were resolved by 8 or 15% SDS–PAGE gels, depending on the sizes of target proteins, transferred to Immobilon-P PVDF membranes (Millipore, Billerica, MA) by electroblotting and then probed with anti-phospho-ERK, anti-ERK, anti-phospho-JNK, anti-JNK, anti-phospho-p38 and anti-p38 antibodies (Cell Signaling Technology, Danvers, MA), anti-p53, anti-catalase, anti-SOD1, anti-SOD2, and anti-β-actin antibodies (Santa Cruz Biotechnology, Santa Cruz, CA). Membranes were incubated with horseradish peroxidase-conjugated secondary antibodies. Blots were developed using an ECL kit (Amersham, Arlington Heights, IL).

Annexin V staining

Apoptosis was determined by staining cells with annexin V-fluorescein isothiocyanate (FITC, PharMingen, San Diego, CA; Ex/Em = 488 nm/519 nm), as previously described (Han et al. 2008c). In brief, 1×10^6 cells in 60 mm culture dish (Nunc) were incubated with 50 μM PG with or without a given MAPK inhibitor for 72 h. Cells were washed twice with cold PBS and then resuspended in 500 μl of binding buffer (10 mM HEPES/NaOH pH 7.4, 140 mM NaCl, 2.5 mM $CaCl_2$) at a concentration of 1×10^6 cells/ml. Five microliters of annexin V-FITC was then added to these cells, which were analyzed using a FACStar flow cytometer (Becton–Dickinson).

Quantification of caspase-3 activity

The activity of caspase-3 was assessed using the caspase-3 colorimetric Assay Kit (R&D systems, Inc. Minneapolis, MN), which is based on the spectrophotometric detection of the color reporter molecule p-nitroanaline (pNA) after cleavage from the labeled substrate DEVD-pNA as an index. In brief, 1×10^6 cells in 60-mm culture dish (Nunc) were incubated with 50 μM PG with or without a given MAPK inhibitor for 72 h. The cells were then washed in PBS and suspended in 5 volumes of lysis buffer (20 mM HEPES pH 7.9, 20% glycerol, 200 mM KCl, 0.5 mM EDTA, 0.5% NP40, 0.5 mM DTT, and 1% protease inhibitor cocktail (from Sigma)). Protein concentrations were determined using the Bradford method. Supernatant samples containing 50 μg of total protein were used for determination of caspase-3 activity. These are added to each well in 96-well microtiter plates (Nunc) with the DEVD-pNA at 37°C for 1 h. The optical density of each well was measured at 405 nm using a microplate reader (Spectra MAX 340, Molecular Devices Co, Sunnyvale, CA, USA). Caspase-3 activity was expressed in arbitrary absorbance units.

Measurement of mitochondrial membrane potential (MMP; $\Delta\Psi_m$)

MMP ($\Delta\Psi_m$) levels were measured using rhodamine 123 fluorescent dye (Sigma–Aldrich Chemical Company; Ex/Em = 485 nm/535 nm) as previously described (Han et al. 2007). In brief, 1×10^6 cells in 60-mm culture dish (Nunc) were incubated with 50 μM PG with or without a given MAPK inhibitor for 72 h. Cells were washed twice with PBS and incubated with rhodamine 123 (0.1 μg/ml) at 37°C for 30 min. Rhodamine 123 staining intensity was determined by flow cytometry (Becton–Dickinson). An absence of rhodamine 123 from cells indicated the loss of MMP ($\Delta\Psi_m$) in As4.1 cells. The MMP ($\Delta\Psi_m$) levels in the cells, excluding MMP ($\Delta\Psi_m$) loss cells, were expressed as the mean fluorescence intensity (MFI), which was calculated by CellQuest software (Becton–Dickinson).

Detection of intracellular ROS and $O_2^{\bullet-}$ levels

Intracellular ROS such as H_2O_2, $^{\bullet}OH$, and $ONOO^{\bullet}$ were detected by means of an oxidation-sensitive fluorescent probe dye, 2′,7′-dichlorodihydrofluorescein diacetate (H_2DCFDA, Invitrogen Molecular Probes, OR; Ex/Em = 495 nm/529 nm) (Han et al. 2008a). As H_2DCFDA is poorly selective for $O_2^{\bullet-}$, dihydroethidium (DHE,

Invitrogen Molecular Probes; Ex/Em = 518 nm/605 nm), which is highly selective for $O_2^{\bullet -}$, was used for its detection. In brief, 1×10^6 cells in 60-mm culture dish (Nunc) were incubated with 50 μM PG with or without a given MAPK inhibitor for 72 h. Cells were then washed in PBS and incubated with 20 μM H_2DCFDA or DHE at 37°C for 30 min according to the instructions of the manufacturer. DCF and DHE fluorescences were detected using a FACStar flow cytometer (Becton–Dickinson). Reactive oxygen species and $O_2^{\bullet -}$ levels were expressed as mean fluorescence intensity (MFI), which was calculated by CellQuest software (Becton–Dickinson).

Detection of the intracellular glutathione

The relative GSH concentrations in As4.1 cells treated with PG and/or a given MAPK inhibitor were analyzed using 5-chloromethylfluorescein diacetate (CMFDA, Invitrogen Molecular Probes; Ex/Em = 522 nm/595 nm), as previously described (Han et al. 2008a). In brief, 1×10^6 cells in 60-mm culture dish (Nunc) were incubated with 50 μM PG with or without a given MAPK inhibitor for 72 h. Cells were then washed with PBS and incubated with 5 μM CMFDA at 37°C for 30 min. CMF fluorescence intensity was determined using a FACStar flow cytometer (Becton–Dickinson). Negative CMF staining (GSH-depleted) cells were expressed as the percent of (−) CMF cells. The CMF levels in cells, excluding GSH-depleted cells, were expressed as mean fluorescence intensity (MFI), which was calculated by CellQuest software (Becton–Dickinson).

Statistical analysis

The results represent the mean of at least three independent experiments (mean ± SD). The data were analyzed using Instat software (GraphPad Prism4, San Diego, CA). The Student's *t*-test or one-way analysis of variance (ANOVA) with post hoc analysis using Tukey's multiple comparison test was used for parametric data. Statistical significance was defined as $P < 0.05$.

Results

Effects of MAPK inhibitors on cell growth, numbers, and their activities in PG-treated As4.1 cells

We examined the effect of MAPK inhibitors on the growth of PG-treated As4.1 cells. Treatment with 50 μM PG decreased the growth of As4.1 cells about 70% at 72 h using an MTT assay (Fig. 1a). All the MAPK inhibitors significantly reduced the growth inhibition of PG (Fig. 1a). In addition, we checked out the viability of PG and/or each

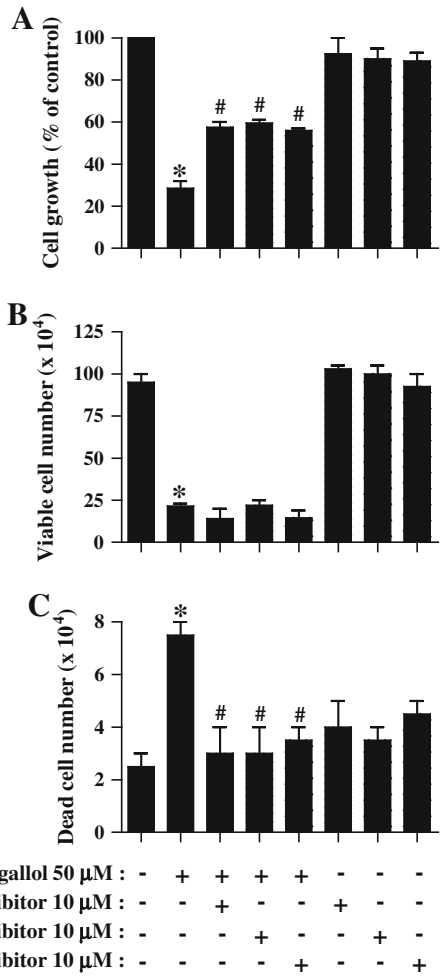

Fig. 1 Effects of MAPK inhibitors on cell growth in PG-treated As4.1 cells. Exponentially growing cells were treated with 50 μM PG for 72 h following 30-min pre-incubation of 10 μM MEK, JNK, or p38 inhibitor. **a** The *graph* shows cell growth changes in As4.1 cells, which was assessed by an MTT assay. **b** and **c** The *graphs* show the viable (trypan blue-negative) and dead (trypan blue-positive) cell numbers in As4.1 cells, respectively. *$P < 0.05$ compared with the control group. # $P < 0.05$ compared with cells treated with PG only

MAPK inhibitor-treated cells using trypan blue cell counting. As shown in Fig. 1b, PG decreased the viable (trypan blue-negative) cell numbers in As4.1 cells, and each MAPK inhibitor did not significantly affect the numbers. PG increased the dead (trypan blue-positive) cell numbers, whereas each MAPK inhibitor significantly reduced the numbers (Fig. 1c). Next, it was determined whether MAPK inhibitors influenced the various stages of the cell cycle of PG-treated cells at 72 h. As shown in Fig. 2, DNA flow cytometric analysis indicated that PG significantly induced a G2 arrest of the cell cycle in As4.1 cells, and each MAPK inhibitor did not change the cell cycle distributions in these cells.

Because the phosphorylation status of specific sites on MAPKs indirectly indicates the quantity of their activities,

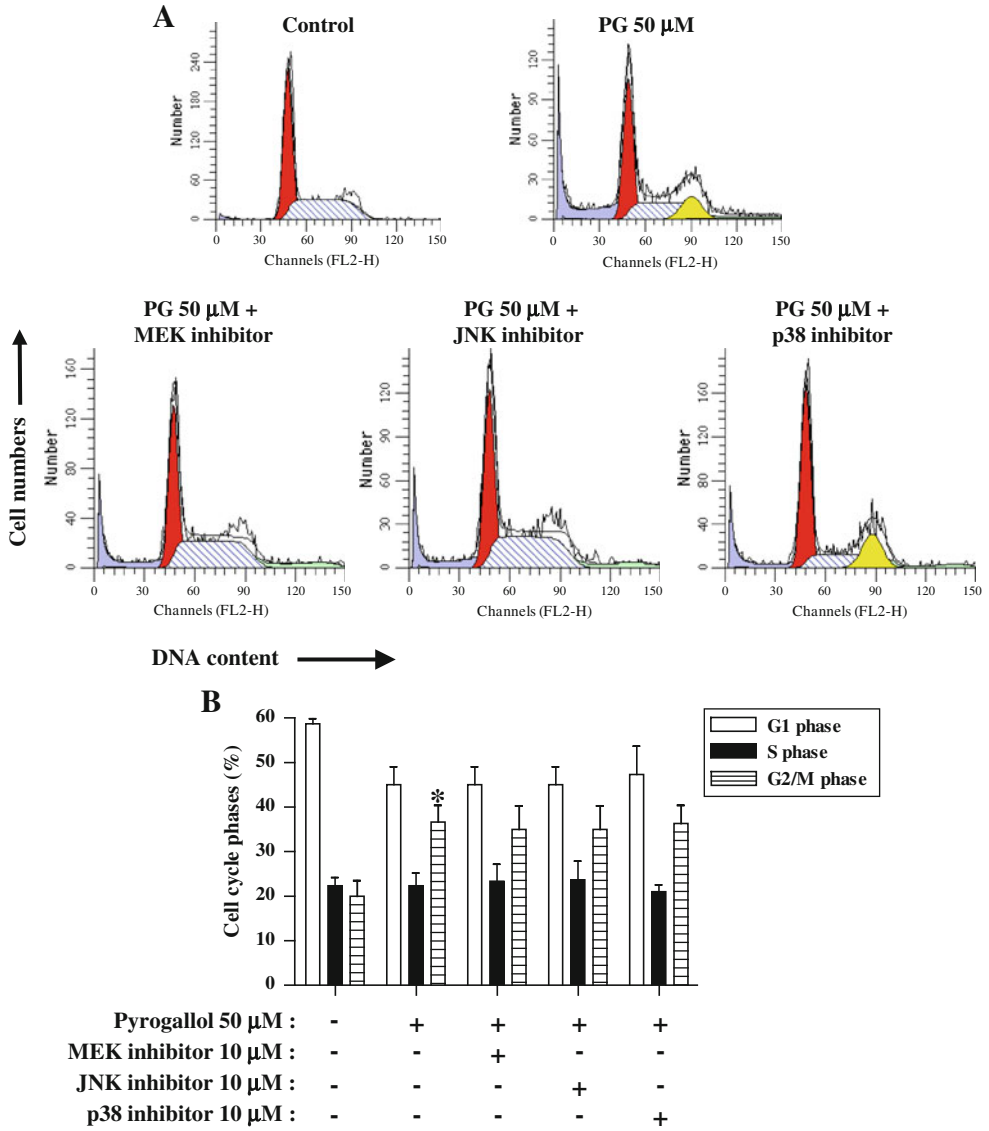

Fig. 2 Effects of MAPK inhibitors on the cell cycle distributions in PG-treated As4.1 cells. Exponentially growing cells were treated with 50 μM PG for 72 h following 30-min pre-incubation of 10 μM MEK, JNK, or p38 inhibitor. The changes in cell cycle phase distribution were assessed by DNA flow cytometric analysis. **a** Each figure shows histograms for cell cycle analysis in As4.1 cells. **b** The *graph* shows the percents of each phase in the cell cycle. $^{*}P < 0.05$ compared with the control group

protein expression of MAPKs and their phosphorylation in PG and/or MAPK inhibitors-treated As4.1 cells were examined by Western blotting at the early time point of 1 h. While PG did not alter the phosphorylation of ERK compared with total ERK expression (Fig. 3a), it increased the phosphorylation of both JNK and p38 compared with their total expression (Fig. 3b, c). MEK inhibitor did not change the phosphorylation of ERK and its total expression in PG-treated As4.1 cells. It decreased the phosphorylation of ERK in As4.1 control cells (Fig. 3a). Each JNK and p38 inhibitor down-regulated the phosphorylation of both JNK and p38 in PG-treated and -untreated As4.1 cells (Fig. 3b, c).

Effects of MAPK inhibitors on apoptosis and MMP ($\Delta\Psi_m$) in PG-treated As4.1 cells

In the current study, PG seemed to induce apoptosis in As4.1 cells at 72 h, as evidenced by sub-G1 and annexin V staining cells (Fig. 4). It was assessed whether each MAPK inhibitor changes PG-induced apoptosis. All the MAPK inhibitors reduced the percent of sub-G1 cells in PG-treated As4.1 cells (Fig. 4a). They also significantly decreased the number of annexin V-FITC-positive cells in PG-treated As4.1 cells, and treatment with p38 inhibitor was strong on that (Fig. 4b). Because p53 protein can induce apoptosis in response to exogenous insults, we examined the effects of

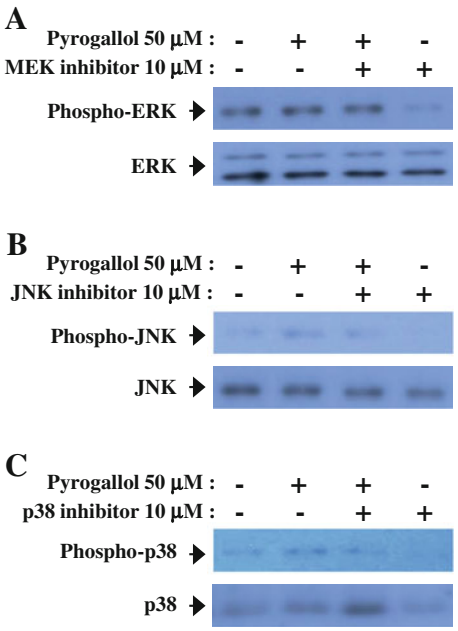

Fig. 3 Effects of MAPK inhibitors on protein expression of MAPKs and their phosphorylation in PG-treated As4.1 cells. Exponentially growing cells were treated with 50 μM PG for 1 h following 30-min pre-incubation of 10 μM MEK, JNK, or p38 inhibitor. Samples (40 μg) of protein extracts were resolved by SDS–PAGE gel, transferred onto the PVDF membranes, and immunoblotted with the indicated antibodies against phospho-ERK and ERK (**a**), phospho-JNK and JNK (**b**), and phospho-p38 and p38 (**c**)

PG and/or each MAPK inhibitor on the expression of p53 protein. As shown in Fig. 5a, PG increased p53 level, and treatment with JNK and p38 inhibitors strongly decreased the p53 level. Next, we examined whether caspase-3 activity is changed by PG and/or each MAPK inhibitor in As4.1 cells. As shown in Fig. 5b, PG significantly increased caspase-3 activity. While both MEK and p38 inhibitor reduced the activity of caspase-3 in PG-treated As4.1 cells, JNK inhibitor did not (Fig. 5b).

In addition, the loss of MMP ($\Delta\Psi_m$) was observed in PG-treated As4.1 cells at 72 h (Fig. 6a, b). All the MAPK inhibitors reduced MMP ($\Delta\Psi_m$) loss in PG-treated As4.1 cells, and p38 inhibitor significantly did (Fig. 6a, b). In relation to MMP ($\Delta\Psi_m$) levels in cells except rhodamine 123-negative cells, PG decreased MMP ($\Delta\Psi_m$) level in As4.1 cells (Fig. 6a, c). All the MAPK inhibitors magnified the reduced MMP ($\Delta\Psi_m$) level in PG-treated As4.1 cells (Fig. 6a, c). They also reduced the basal MMP ($\Delta\Psi_m$) level in As4.1 control cells (Fig. 6a, c).

Effects of MAPK inhibitors on ROS and GSH levels in PG-treated As4.1 cells

Next, it was determined whether the levels of intracellular ROS in PG-treated As4.1 cells were changed by each inhibitor of MAPK at 72 h. Intracellular ROS (DCF) level such as H_2O_2 was slightly increased in PG-treated As4.1 cells (Fig. 7a). All the MAPK inhibitors did not alter the level in these cells (Fig. 7a). They all increased the basal ROS level in As4.1 control cells (Fig. 7a). The red fluorescence derived from DHE reflecting intracellular $O_2^{\bullet-}$ level was increased in PG-treated As4.1 cells (Fig. 7b). All the MAPK inhibitors significantly reduced the $O_2^{\bullet-}$ level, and none of the inhibitors affected $O_2^{\bullet-}$ basal levels in As4.1 control cells (Fig. 7b).

SOD, which catalyzes the dismutation of $O_2^{\bullet-}$ into H_2O_2 and molecular oxygen, is one of the most important anti-oxidative enzymes. Catalase then metabolizes H_2O_2 to O_2 and H_2O. (Wilcox 2002). As shown in Fig. 7c, PG slightly reduced the expression level of catalase but did not alter the expression levels of Cu/Zn-SOD and Mn-SOD. All the MAPK inhibitors intensified the reduced level of catalase

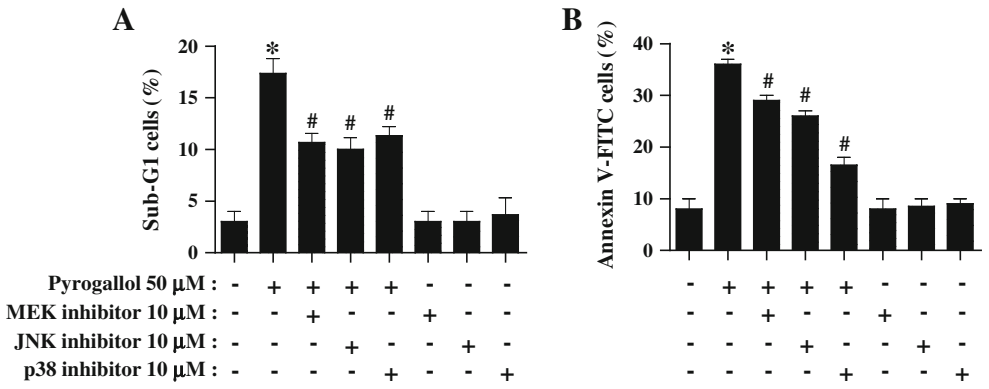

Fig. 4 Effects of MAPK inhibitors on apoptosis in PG-treated As4.1 cells. Exponentially growing cells were treated with 50 μM PG for 72 h following 30-min pre-incubation of 10 μM MEK, JNK, or p38 inhibitor. Sub-G1 and annexin V-FITC cells were measured with a FACStar flow cytometer, respectively. **a** and **b** *Graphs* show the percents of sub-G1 cells and annexin V-positive staining cells, respectively. *$P < 0.05$ compared with the control group. #$P < 0.05$ compared with cells treated with PG only

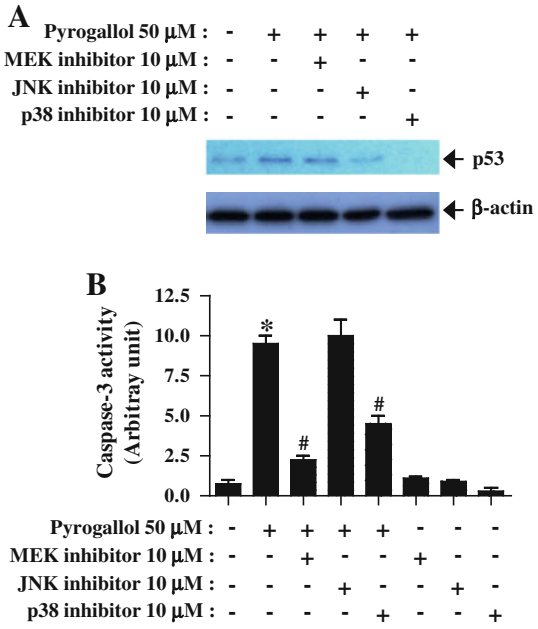

Fig. 5 Effects of MAPK inhibitors on the levels of p53 expression and caspase-3 activity in PG-treated As4.1 cells. Exponentially growing cells were treated with 50 μM PG for 72 h following 30-min pre-incubation of 10 μM MEK, JNK, or p38 inhibitor. **a** Samples (40 μg) of protein extracts were resolved by SDS–PAGE gel, transferred onto PVDF membranes, and immunoblotted with the indicated antibodies against p53 and *β*-actin. **b** The graph shows the changes in caspase-3 activity in samples containing 50 μg of total protein. $*P < 0.05$ compared with the control group. $\# P < 0.05$ compared with cells treated with PG only

in PG-treated As4.1 cells, and p38 inhibitor showed very strong effect (Fig. 7c). They did not alter the level of Mn-SOD in PG-treated As4.1 cells (Fig. 7c). In relation to Cu/Zn-SOD, only p38 inhibitor reduced this level in PG-treated As4.1 cells (Fig. 7c).

When the changes in GSH levels in As4.1 cells treated with PG and/or each MAPK inhibitor were investigated, PG increased the number of GSH-depleted cells in As4.1 cells about 33% compared with that of control cells at 72 h (Fig. 7d). All the MAPK inhibitors significantly reduced the GSH-depleted cell numbers (Fig. 7d). Treatment with p38 inhibitor increased GSH-depleted cell number in As4.1 control cells (Fig. 7d).

Discussion

PG inhibited As4.1 cell growth and induced apoptosis, which accompanied by the loss of MMP ($\Delta\Psi_m$). All the MAPK inhibitors significantly attenuated the growth inhibition and apoptosis of PG-treated As4.1 cells. Each MAPK inhibitor did not significantly influence the cell viability. These results suggest that the attenuation of PG-induced As4.1 cell growth inhibition by MAPK inhibitors results from the prevention of cell death rather than the increase in cell proliferation. In fact, DNA flow cytometric analysis indicated that PG significantly induced a G2 arrest of the cell cycle in As4.1 cells, and each MAPK inhibitor did not change the cell cycle distributions in these cells. Thus, the signaling of MAPKs might not tightly regulate the cell cycle distributions and cell proliferations in PG-treated As4.1 cells.

ERK activation has a pro-survival function rather than pro-apoptotic effects (Henson and Gibson 2006; Rygiel et al. 2008). According to our current results, PG did not alter the phosphorylation of ERK in As4.1 cells. MEK inhibitor also did not influence the phosphorylation status of ERK in PG-treated As4.1 cells. However, because MEK inhibitor significantly prevented apoptosis in PG-treated As4.1 cells, the signaling of ERK did not seem to be involved in PG-induced apoptosis in As4.1 cells. Probably, MEK inhibitor seemed to rescue As4.1 cells from PG insults via affecting other signaling independent of ERK. In relation to JNK and p38, PG increased the activities of both JNK and p38. JNK and p38 inhibitors down-regulated their activities in PG-treated As4.1 cells, which was accompanied by the prevention of apoptosis. Therefore, our data support the notion that that the activation of JNK and p38 generally leads to apoptosis (Gomez-Lazaro et al. 2007; Nagai et al. 2007; Hsin et al. 2008; Mao et al. 2008). Especially, signaling of p38 was strongly related to PG-induced apoptosis in As4.1 cells. Moreover, PG increased the level of p53 protein, which is positively involved in apoptosis. JNK and p38 inhibitors strongly decreased the p53 level. These results suggest that the blocking of JNK and p38 signaling by their inhibitors attenuates apoptosis pathway in PG-treated As4.1 cells via regulating p53 protein status. Moreover, both MEK and p38 inhibitor reduced the activity of caspase-3 in PG-treated As4.1 cells, which implied that caspase-3 plays an important role in regulating the induction of apoptosis in these cells. However, JNK inhibitor showing anti-apoptotic effect did not down-regulate the activity of caspase-3 in PG-treated As4.1 cells. Therefore, other executed caspases besides caspase-3 also seemed to be strongly involved in apoptosis in As4.1 cells. Each MAPK signaling might differently regulate caspase-3 activation in PG-treated As4.1 cells.

A number of studies suggested that the serine/threonine kinase of MAPKs can be regulated by ROS (Gomez-Lazaro et al. 2007; Nagai et al. 2007; Hsin et al. 2008; Mao et al. 2008). Pyrogallol can disturb the natural oxidation and reduction equilibrium in cells via $O_2^{\bullet -}$ generation. The increased patterns of $O_2^{\bullet -}$ level by pyrogallol were reported in the pheochromocytoma PC12 cells (Yamada et al. 2003) and human neuroblastoma SH-SY5Y cells (Poulose et al. 2005). Intracellular ROS (DCF) level such as H_2O_2 was slightly increased in PG-treated As4.1 cells. All the MAPK

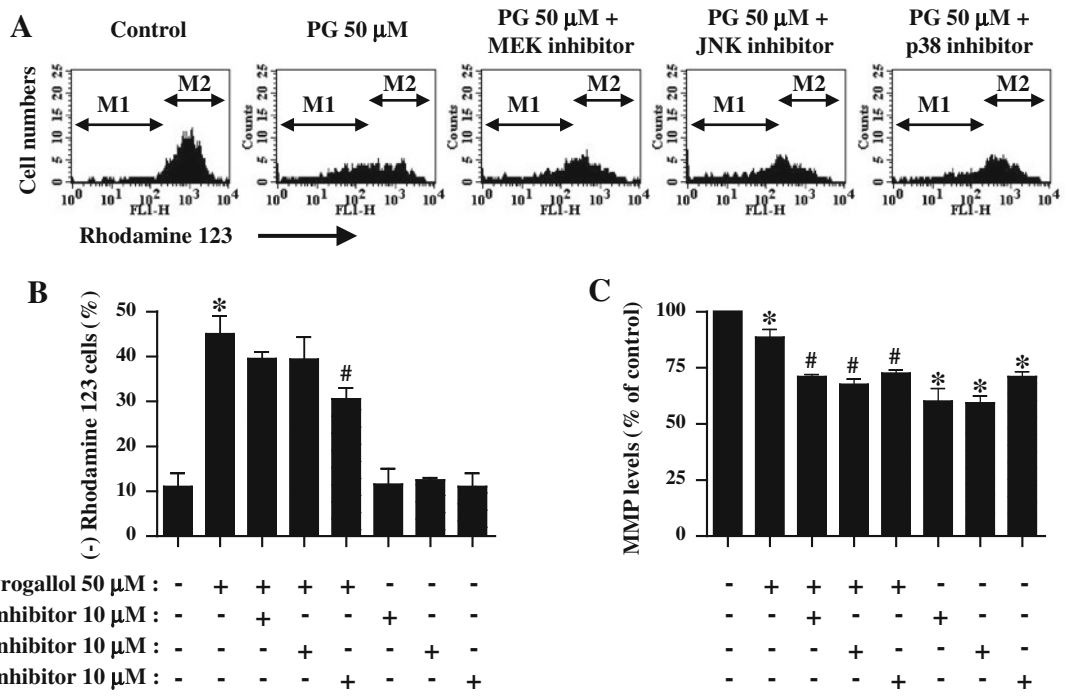

Fig. 6 Effects of MAPK inhibitors on MMP ($\Delta\Psi_m$) in PG-treated As4.1 cells. Exponentially growing cells were treated with 50 μM PG for 72 h following 30-min pre-incubation of 10 μM MEK, JNK, or p38 inhibitor. **a** MMP ($\Delta\Psi_m$) in As4.1 cells was measured with a FACStar flow cytometer. **b** and **c** *Graphs* show the percent of rhodamine 123-negative (MMP ($\Delta\Psi_m$) loss) cells (M1 region in **a**) (**b**) and MMP ($\Delta\Psi_m$) levels (%) compared with As4.1 control cells (M2 region in **a**) (**c**). $^*P < 0.05$ compared with the control group. # $P < 0.05$ compared with cells treated with PG only

inhibitors did not alter the level in these cells. Catalase protein levels in PG and/or MAPK inhibitors-treated As4.1 cells were not correlated with the change in ROS (DCF) level. MAPK inhibitors also increased the basal ROS level in As4.1 control cells without apoptosis induction. These data suggest that the changes in ROS (DCF) levels by PG and/or MAPK inhibitors are not tightly correlated with cell death and are not closely regulated by catalase expression in As4.1 cells. When we detected the intracellular $O_2^{\bullet-}$ levels in PG-treated As4.1 cells, PG strongly increased $O_2^{\bullet-}$ level. It is reported that ROS formation may cause mitochondrial dysfunction and subsequent cytochrome c release, which leads to cell viability loss (Qiu et al. 2000; Ling et al. 2003). The collapse of MMP ($\Delta\Psi_m$) occurs during apoptosis (Yang et al. 1997). Correspondingly, PG induced the loss of MMP ($\Delta\Psi_m$) and decreased MMP ($\Delta\Psi_m$) levels in As4.1 cells. All the MAPK inhibitors reduced $O_2^{\bullet-}$ level and the loss of MMP ($\Delta\Psi_m$) in PG-treated As4.1 cells. Treatment with p38 inhibitor showed very strong effects. These results imply that the loss of MMP ($\Delta\Psi_m$) following treatment with PG leads to apoptosis in As4.1 cells, and the signaling of MAPKs positively affects MMP ($\Delta\Psi_m$) loss in PG-treated As4.1 cells. In addition, our data suggest that the changes in the intracellular $O_2^{\bullet-}$ levels are correlated with apoptosis in PG-treated As4.1 cells. In relation to $O_2^{\bullet-}$ levels, the increase in $O_2^{\bullet-}$ level in PG-treated As4.1 cells probably resulted from its enhanced production rather than the decreased activity of SOD, since PG did not change the levels of Cu/Zn- and Mn-SOD proteins and their activity significantly (Park et al. 2007a). The decreased effects of MAPK inhibitors on $O_2^{\bullet-}$ level in PG-treated As4.1 cells also might not be regulated by expression level of Cu/Zn- and Mn-SOD proteins. Even though p38 inhibitor reduced Cu/Zn-SOD protein level in PG-treated As4.1 cells, this did not increase $O_2^{\bullet-}$ level. Concerning MMP ($\Delta\Psi_m$) level, all the MAPK inhibitors magnified the reduced MMP ($\Delta\Psi_m$) level in PG-treated As4.1 cells. They also reduced the basal MMP ($\Delta\Psi_m$) level in As4.1 control cells. The changes in MMP ($\Delta\Psi_m$) level by PG and/or MAPK inhibitors might not be related to apoptosis in As4.1 cells. Because the magnitude of the MMP ($\Delta\Psi_m$) level reflects or affects metabolic workload and the redox potential of the electron carriers of the respiratory chain, the changes in MMP ($\Delta\Psi_m$) level by PG and/or MAPK inhibitors seemed to affect ROS levels including $O_2^{\bullet-}$.

Cellular GSH can regulate cell growth and apoptosis (Poot et al. 1995; Schnelldorfer et al. 2000). Our current data showed that PG increased the number of GSH-depleted cells in As4.1 cells. All the MAPK inhibitors significantly reduced the GSH-depleted cell numbers. Treatment with p38 inhibitor showing the strong anti-apoptotic effect on PG-induced apoptosis in As4.1 cells also efficiently prevented the GSH depletion. Our data support the notion that the intracellular

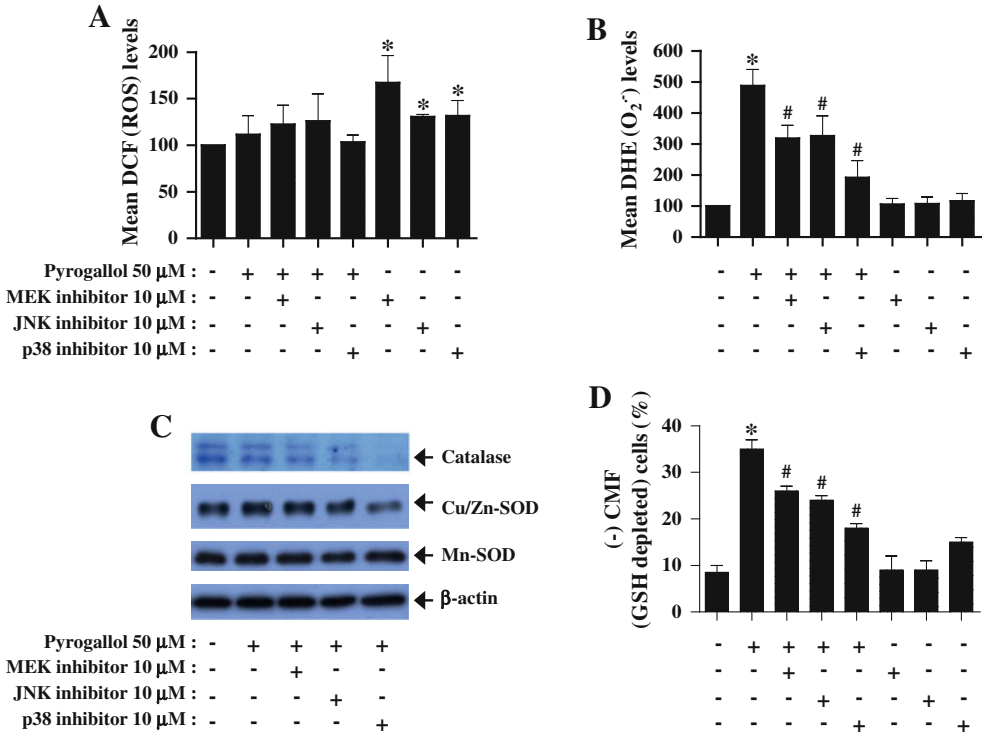

Fig. 7 Effects of MAPK inhibitors on ROS levels in PG-treated As4.1 cells. Exponentially growing cells were treated with 50 μM PG for 72 h following 30-min pre-incubation of 10 μM MEK, JNK, or p38 inhibitor. **a** and **b** ROS levels in As4.1 cells were measured using a FACStar flow cytometer. *Graphs* indicate DCF (ROS) levels (%) compared with control cells (**a**) and DHE ($O_2^{\bullet-}$) levels (%) compared with control cells (**b**). **c** Samples (40 μg) of protein extracts were resolved by SDS–PAGE gel, transferred onto the PVDF membranes, and immunoblotted with the indicated antibodies against catalase, Cu/Zn-SOD, Mn-SOD, and *β*-actin. D: GSH levels in As4.1 cells were measured using a FACStar flow cytometer. *Graph* shows the percent of (−) CMF (GSH-depleted) cells. * $P < 0.05$ compared with the control group. # $P < 0.05$ compared with cells treated with PG only

GSH content has a decisive effect on anticancer drug-induced apoptosis (Higuchi 2004; Estrela et al. 2006), but it is not sufficient to predict cell death correctly, since p38 alone increased GSH-depleted cell number in As4.1 control cells without apoptosis induction.

Conclusively, MAPK inhibitors attenuated cell growth inhibition and apoptosis in PG-treated As4.1 cells. The changes in $O_2^{\bullet-}$ and GSH content levels by PG and/or MAPK inhibitors seemed to affect the growth and death of As4.1 cells.

Acknowledgments This research was supported by a grant of the Korea Healthcare Technology R&D Project, Ministry for Health, Welfare & Family Affairs and Republic of Korea (A084194).

Conflict of interest statement None declared.

References

Baran CP, Zeigler MM, Tridandapani S, Marsh CB (2004) The role of ROS and RNS in regulating life and death of blood monocytes. Curr Pharm Des 10:855–866

Blenis J (1993) Signal transduction via the MAP kinases: proceed at your own RSK. Proc Natl Acad Sci U S A 90:5889–5892

Bubici C, Papa S, Pham CG, Zazzeroni F, Franzoso G (2006) The NF-kappaB-mediated control of ROS and JNK signaling. Histol Histopathol 21:69–80

Chen TJ, Jeng JY, Lin CW, Wu CY, Chen YC (2006) Quercetin inhibition of ROS-dependent and -independent apoptosis in rat glioma C6 cells. Toxicology 223:113–126

Dasmahapatra G, Rahmani M, Dent P, Grant S (2006) The tyrphostin adaphostin interacts synergistically with proteasome inhibitors to induce apoptosis in human leukemia cells through a reactive oxygen species (ROS)-dependent mechanism. Blood 107:232–240

Estrela JM, Ortega A, Obrador E (2006) Glutathione in cancer biology and therapy. Crit Rev Clin Lab Sci 43:143–181

Genestra M (2007) Oxyl radicals, redox-sensitive signalling cascades and antioxidants. Cell Signal 19:1807–1819

Gomez-Lazaro M et al (2007) Reactive oxygen species and p38 mitogen-activated protein kinase activate Bax to induce mitochondrial cytochrome c release and apoptosis in response to malonate. Mol Pharmacol 71:736–743

Guyton KZ, Liu Y, Gorospe M, Xu Q, Holbrook NJ (1996) Activation of mitogen-activated protein kinase by H2O2. Role in cell survival following oxidant injury. J Biol Chem 271:4138–4142

Han YH, Kim SZ, Kim SH, Park WH (2007) Arsenic trioxide inhibits growth of As4.1 juxtaglomerular cells via cell cycle arrest and

caspase-independent apoptosis. Am J Physiol Renal Physiol 293:F511–F520

Han YH, Kim SH, Kim SZ, Park WH (2008a) Caspase inhibitor decreases apoptosis in pyrogallol-treated lung cancer Calu-6 cells via the prevention of GSH depletion. Int J Oncol 33:1099–1105

Han YH, Kim SW, Kim SH, Kim SZ, Park WH (2008b) 2, 4-dinitrophenol induces G1 phase arrest and apoptosis in human pulmonary adenocarcinoma Calu-6 cells. Toxicol In Vitro 22:659–670

Han YH, Kim SZ, Kim SH, Park WH (2008c) Apoptosis in pyrogallol-treated Calu-6 cells is correlated with the changes of intracellular GSH levels rather than ROS levels. Lung Cancer 59:301–314

Han YH, Kim SZ, Kim SH, Park WH (2009) Pyrogallol inhibits the growth of lung cancer Calu-6 cells via caspase-dependent apoptosis. Chem Biol Interact 177:107–114

Henson ES, Gibson SB (2006) Surviving cell death through epidermal growth factor (EGF) signal transduction pathways: implications for cancer therapy. Cell Signal 18:2089–2097

Higuchi Y (2004) Glutathione depletion-induced chromosomal DNA fragmentation associated with apoptosis and necrosis. J Cell Mol Med 8:455–464

Hsin YH, Chen CF, Huang S, Shih TS, Lai PS, Chueh PJ (2008) The apoptotic effect of nanosilver is mediated by a ROS- and JNK-dependent mechanism involving the mitochondrial pathway in NIH3T3 cells. Toxicol Lett 179:130–139

Kusuhara M et al (1998) p38 Kinase is a negative regulator of angiotensin II signal transduction in vascular smooth muscle cells: effects on Na +/H + exchange and ERK1/2. Circ Res 83:824–831

Ling YH, Liebes L, Zou Y, Perez-Soler R (2003) Reactive oxygen species generation and mitochondrial dysfunction in the apoptotic response to Bortezomib, a novel proteasome inhibitor, in human H460 non-small cell lung cancer cells. J Biol Chem 278:33714–33723

Mao X, Yu CR, Li WH, Li WX (2008) Induction of apoptosis by shikonin through a ROS/JNK-mediated process in Bcr/Abl-positive chronic myelogenous leukemia (CML) cells. Cell Res 18:879–888

Moreno-Manzano V, Ishikawa Y, Lucio-Cazana J, Kitamura M (2000) Selective involvement of superoxide anion, but not downstream compounds hydrogen peroxide and peroxynitrite, in tumor necrosis factor-alpha-induced apoptosis of rat mesangial cells. J Biol Chem 275:12684–12691

Nagai H, Noguchi T, Takeda K, Ichijo H (2007) Pathophysiological roles of ASK1-MAP kinase signaling pathways. J Biochem Mol Biol 40:1–6

Park WH et al (2000) Arsenic trioxide-mediated growth inhibition in MC/CAR myeloma cells via cell cycle arrest in association with induction of cyclin-dependent kinase inhibitor, p21, and apoptosis. Cancer Res 60:3065–3071

Park WH, Han YH, Kim SH, Kim SZ (2007a) Pyrogallol, ROS generator inhibits As4.1 juxtaglomerular cells via cell cycle arrest of G2 phase and apoptosis. Toxicology 235:130–139

Park WH, Han YW, Kim SH, Kim SZ (2007b) A superoxide anion generator, pyrogallol induces apoptosis in As4.1 cells through the depletion of intracellular GSH content. Mutat Res 619:81–92

Poot M, Teubert H, Rabinovitch PS, Kavanagh TJ (1995) De novo synthesis of glutathione is required for both entry into and progression through the cell cycle. J Cell Physiol 163:555–560

Poulose SM, Harris ED, Patil BS (2005) Citrus limonoids induce apoptosis in human neuroblastoma cells and have radical scavenging activity. J Nutr 135:870–877

Qiu JH, Asai A, Chi S, Saito N, Hamada H, Kirino T (2000) Proteasome inhibitors induce cytochrome c-caspase-3-like protease-mediated apoptosis in cultured cortical neurons. J Neurosci 20:259–265

Rygiel TP, Mertens AE, Strumane K, van der Kammen R, Collard JG (2008) The Rac activator Tiam1 prevents keratinocyte apoptosis by controlling ROS-mediated ERK phosphorylation. J Cell Sci 121:1183–1192

Saeki K, Hayakawa S, Isemura M, Miyase T (2000) Importance of a pyrogallol-type structure in catechin compounds for apoptosis-inducing activity. Phytochemistry 53:391–394

Sawada M et al (2001) p53 regulates ceramide formation by neutral sphingomyelinase through reactive oxygen species in human glioma cells. Oncogene 20:1368–1378

Schnelldorfer T, Gansauge S, Gansauge F, Schlosser S, Beger HG, Nussler AK (2000) Glutathione depletion causes cell growth inhibition and enhanced apoptosis in pancreatic cancer cells. Cancer 89:1440–1447

Sigmund CD et al (1990) Isolation and characterization of renin-expressing cell lines from transgenic mice containing a renin-promoter viral oncogene fusion construct. J Biol Chem 265:19916–19922

Simon HU, Haj-Yehia A, Levi-Schaffer F (2000) Role of reactive oxygen species (ROS) in apoptosis induction. Apoptosis 5:415–418

Wallach-Dayan SB, Izbicki G, Cohen PY, Gerstl-Golan R, Fine A, Breuer R (2006) Bleomycin initiates apoptosis of lung epithelial cells by ROS but not by Fas/FasL pathway. Am J Physiol Lung Cell Mol Physiol 290:L790–L796

Wilcox CS (2002) Reactive oxygen species: roles in blood pressure and kidney function. Curr Hypertens Rep 4:160–166

Yamada J et al (2003) Cell permeable ROS scavengers, Tiron and Tempol, rescue PC12 cell death caused by pyrogallol or hypoxia/reoxygenation. Neurosci Res 45:1–8

Yang J et al (1997) Prevention of apoptosis by Bcl-2: release of cytochrome c from mitochondria blocked. Science 275:1129–1132

Zelko IN, Mariani TJ, Folz RJ (2002) Superoxide dismutase multigene family: a comparison of the CuZn-SOD (SOD1), Mn-SOD (SOD2), and EC-SOD (SOD3) gene structures, evolution, and expression. Free Radic Biol Med 33:337–349

Zorov DB, Juhaszova M, Sollott SJ (2006) Mitochondrial ROS-induced ROS release: An update and review. Biochim Biophys Acta 1757:509–517